Research Square

Preprints are preliminary reports that have not undergone peer review.
They should not be considered conclusive, used to inform clinical practice,
or referenced by the media as validated information.

Adaptive Dynamic Site Selection for Emergency Logistics Using SSA-MOPSO with a Multi-Period Multi-Objective Optimization Framework

Guobin Gu
Naresuan University
Longtang Ning
Naresuan University
Benxioa Lou
Central South University
Qinwei Hu
Guangxi Vocational and Technical College of Communications
Junhui Luo
Guangxi Vocational and Technical College of Communications
Shixuan Zhou
Nanning University
Boonsub Panichakarn
boonsubp@nu.ac.th
Naresuan University

Article

Keywords: Emergency Logistics, Dynamic Site Selection, Multi-Period Optimization, Multi-Objective Optimization, SSA-MOPSO, EWM-CRITIC

Posted Date: September 17th, 2026

DOI: https://doi.org/10.21203/rs.3.rs-10887496/v1

License: This work is licensed under a Creative Commons Attribution 4.0 International License.
Read Full License

Additional Declarations: No competing interests reported.

Adaptive Dynamic Site Selection for Emergency Logistics Using SSA-MOPSO with a Multi-Period Multi-Objective Optimization Framework

Guobin Gu [1],Longtang Ning [1,4], Benxiao Lou [2],Qinwei Hu[3] , Junhui Luo[3],Shixuan Zhou[4] , BOONSUB PANICHAKARN[1,*]

[1]Faculty of Logistics and Digital Supply Chain, Naresuan University, Phitsanulok 65000, Thailand;
[2]School of Traffic and Transportation Engineering, Central South University, Changsha 410075, China;
[3]School of Intelligent Transportation Engineering,Guangxi Vocational and Technical College of Communications, Nanning 530216, China;
[4]Guangxi Key Laboratory of International Join for China-ASEAN Comprehensive Transportation, Nanning University, Nanning 530200, China;
[*] Corresponding author: BOONSUB PANICHAKARN boonsubp@nu.ac.th (B.P.)

Abstract A public health emergency will cause a rapid shortage of emergency supplies, and it is easy to create an uneven distribution, making scheduling difficult. This research presents a self-adaptive dynamic site selection framework, which combines a multi-period multi-objective site selection model with an enhanced multi-objective particle group optimization (SSA-MOPSO) algorithm. Minimize total logistics cost and delivery distance, and maximize comprehensive satisfaction. The SSA algorithm adapts the key parameters of the MOPSO algorithm according to the changes in the non-control solution quality. In addition, this study also uses an improved EWM-CRITIC method to sort the candidate facilities and determine their priority activation order during different emergencies. The hospital's medical supplies scheduling data was evaluated. Compared with the traditional MOPSO algorithm, the SSA-MOPSO algorithm reduced the total delivery distance by 10,406,195 kilometers and the total cost by 72,843,371 yuan, while improving the overall satisfaction by 0.689%.NSGA-II, MOGWO and MOPSO algorithm. The EWM-CRITIC algorithm identifies Wuhan Red Cross Hospital as the initial site with the highest priority, and the overall weight is 0.165. The results show that, in the case of demand and capacity changing over time, combining dynamic site selection modeling, adaptive multi-objective optimization and target site priority ranking can effectively solve the emergency logistics problem.

Keywords Emergency Logistics; Dynamic Site Selection; Multi-Period Optimization; Multi-Objective Optimization; SSA-MOPSO; EWM-CRITIC

1.Introduction

Public health emergencies impose substantial pressure on logistics systems because demand for medical supplies can increase abruptly, shift geographically, and fluctuate considerably over short periods. During the early stages of an outbreak, shortages may emerge simultaneously across multiple locations, while subsequent stages may experience sustained but uneven demand before conditions gradually stabilize. These temporal and spatial variations make emergency medical supply allocation considerably more complex than conventional logistics planning. Under such conditions, the location and scheduling of emergency distribution centers directly affect response efficiency, resource utilization, distribution distance, and demand fulfillment. Developing facility-location strategies that can adapt to changing demand is therefore a critical issue in emergency logistics management.

To address these issues, this study develops an adaptive dynamic site-selection framework for emergency logistics based on SSA-MOPSO. The principal contributions are fourfold. First, the study develops a multi-period emergency logistics location model that simultaneously considers cost, distribution distance, and comprehensive satisfaction, allowing facility configurations to respond dynamically to changes in demand and capacity. Second, it proposes an adaptive SSA-MOPSO algorithm in which SSA dynamically

regulates key MOPSO parameters, complemented by elite opposition-based learning and density-adaptive grid management to improve convergence and solution diversity. Third, an improved EWM-CRITIC procedure is integrated with the optimization framework to prioritize candidate facilities while accounting for the operational continuity required by emergency medical supplies with specific storage conditions. Fourth, the framework is evaluated using actual Wuhan medical supply dispatch data and comparative algorithm experiments, providing empirical evidence of its effectiveness for dynamic site-selection and material-allocation decisions.

Overall, this study conceptualizes emergency logistics site selection as an integrated multi-period, multi-objective, and sequential decision problem rather than a static facility-location task. By linking dynamic location modeling, adaptive multi-objective optimization, and objective site prioritization, the proposed framework provides a systematic approach for adjusting emergency distribution networks as demand and capacity conditions evolve.

2.Literature Review

2.1 A. Model Formulation and Complexity Analysis of the Emergency Logistics Location–Path Problem

Emergency logistics location–routing problems involve interdependent decisions concerning facility location, transportation routing, material allocation, and service coverage. Distribution-center selection determines feasible routing and allocation alternatives, while demand, capacity, and transportation requirements influence the suitability of candidate facilities. The interaction among these decisions, together with operational constraints, results in a computationally complex optimization problem.

Emergency logistics location and allocation problems are generally characterized as NP-hard. Wang et al. [1] noted that conventional exact methods may become computationally inefficient as problem scale and constraint complexity increase. Consequently, metaheuristic approaches, including genetic algorithms, particle swarm optimization, and simulated annealing, have been increasingly applied to large-scale emergency logistics problems where facility-location decisions must be coordinated with material allocation and distribution.

The complexity of emergency network design is further reflected in the diversity of operational constraints. He et al. [2] developed a bi-objective emergency logistics network model for pandemic conditions that considers relaxed inventory and time costs within a road–rail intermodal framework. Their formulation integrates distribution-center location and coverage-path allocation while incorporating supply–demand balance, routing, and capacity constraints, demonstrating that emergency network design extends beyond a conventional facility-location problem.

Uncertainty introduces an additional layer of complexity. Zhang and Li [3] modeled stochastic material demand using a normal distribution and developed an emergency facility location–routing model incorporating road reliability, with Monte Carlo simulation applied to evaluate stochastic variables within chance constraints. Their work highlights the importance of jointly considering uncertain demand and transportation reliability. Similarly, Teng et al. [4] employed LINGO and a straight-line distance matrix to prioritize facilities near high-weight demand points for earthquake emergency preparedness. Although proximity improved service efficiency, capacity limitations and demand variation indicate that the nearest facility may not always represent the most appropriate location.

The combinatorial nature of emergency logistics is further demonstrated by Yang, Y. [5], who formulated cloud-based emergency distribution as a multi-source, multi-center, and multi-demand-point transportation problem and employed a genetic algorithm for its solution. Hu et al. [6] likewise characterized emergency evacuation routing as NP-hard and distinguished between microscopic simulation and macroscopic

optimization approaches.

Collectively, these studies establish that emergency logistics location decisions are closely interconnected with routing and material allocation, are affected by uncertainty in demand and transportation conditions, and involve substantial computational complexity. These characteristics provide the methodological basis for a multi-period dynamic location framework in which demand, facility capacity, service coverage, and allocation decisions are considered jointly.

2.2 B. Application of Multi-Objective Optimization in Emergency Facility Site Selection and Re-source Allocation

Emergency logistics decisions inherently involve conflicting objectives. Concentrating operations at fewer facilities may reduce operating costs, whereas minimizing distribution distance or rescue time may require a more decentralized network. Similarly, improving coverage or service satisfaction can increase resource requirements. Multi-objective optimization is therefore well suited to emergency facility-location problems because it preserves trade-offs among competing criteria rather than reducing system performance to a single objective.

Zhou, B [7] developed a dual-objective model incorporating comprehensive cost and rescue time. Their intelligent emergency logistics approach achieved a mini-mum comprehensive cost of CNY 6,879 and a minimum rescue time of 4.82 h, representing reductions of approximately 22.1% and 49.5%, respectively, compared with the traditional approach. These findings illustrate the value of simultaneously considering multiple performance criteria in emergency logistics decision-making.

From a broader logistics-network perspective, Wang et al. [10] emphasized that node selection and transportation strategies should jointly consider cost, efficiency, profitability, utilization, robustness, and demand priority. This further supports the use of multi-objective approaches when logistics facilities must satisfy multiple operational requirements simultaneously.

Overall, prior research establishes the suitability of multi-objective optimization for logistics site selection while highlighting the dependence of solution quality on convergence, global search capability, and diversity preservation. Accordingly, this study retains MOPSO as the Pareto-based optimization framework while addressing its limitations through SSA-based adaptive parameter adjustment, elite opposition-based learning, and density-adaptive grid management, thereby enhancing its applicability to dynamic, multi-period emergency logistics decisions.

2.3 Research gaps and theoretical framework

Facility optimization alone does not fully resolve emergency site-selection decisions. Even when optimization generates feasible or non-dominated alternatives, decision-makers must determine the relative priority of candidate facilities for implementation. This requires a comprehensive evaluation framework that integrates operational outcomes with facility characteristics and can accommodate changing emergency conditions.

Accordingly, prior research establishes the computational complexity of emergency location-routing problems [1–6], the applicability of multi-objective optimization and MOPSO to facility-location decisions [7–10], and the importance of systematic candidate-site evaluation [8-11]. Building on these foundations, this study integrates dynamic multi-period location optimization, adaptive multi-objective search, and objective site-priority evaluation. Specifically, the proposed framework combines a mul-ti-period model minimizing total cost and distribution distance while maximizing comprehensive satisfaction with SSA-enhanced MOPSO and an improved EWM-CRITIC procedure. This integration enables candidate facilities to be evaluated under changing emergency conditions while establishing their activation priority as demand and capacity requirements evolve.

3.Methodology

3.1 Technical Approach

This study develops an adaptive multi-period site-selection framework for emergency medical supply distribution centers under dynamically changing demand conditions, using Wuhan, China, as the empirical setting. As illustrated in Figure 1, the framework integrates dynamic multi-objective location optimization, SSA-enhanced MOPSO, and comprehensive site evaluation within a sequential decision process.

This paper constructs a research framework for UAV emergency logistics site selection and material distribution, targeting the issues of time-varying demand for emergency medical supplies, mismatch between site service capacity and actual demand, and the limited adaptability of traditional static location methods. First, considering the demand changes across different emergency phases, site capacities, and transport conditions, a multi-period dynamic location-allocation model is established. Under constraints including demand-capacity matching, service coverage, and flow conservation, the model determines the activation scheme for emergency logistics sites and the corresponding material allocation plan. This multi-objective framework minimizes cost and distance while maximizing satisfaction, embeds SSA in MOPSO with adaptive tuning for better convergence and diversity, uses EWM-CRITIC to prioritize site activation, and defines UAV allocation and service. It overcomes static model limits and supports dynamic emergency logistics decisions.

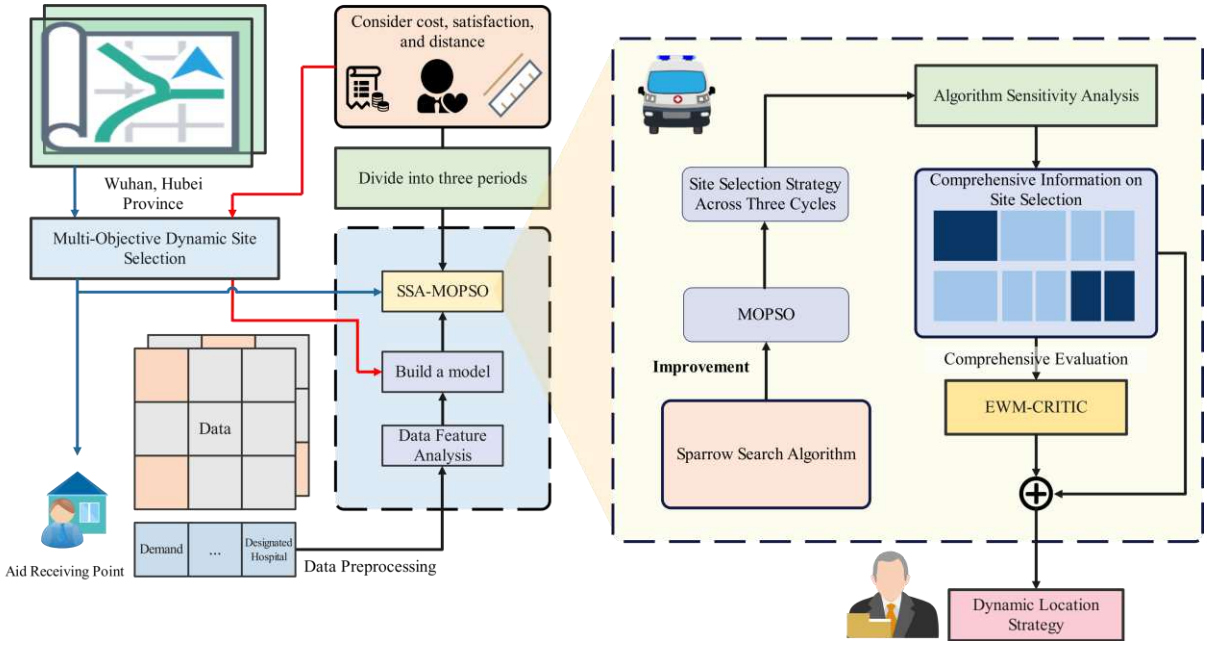


Figure 1. Research process map.

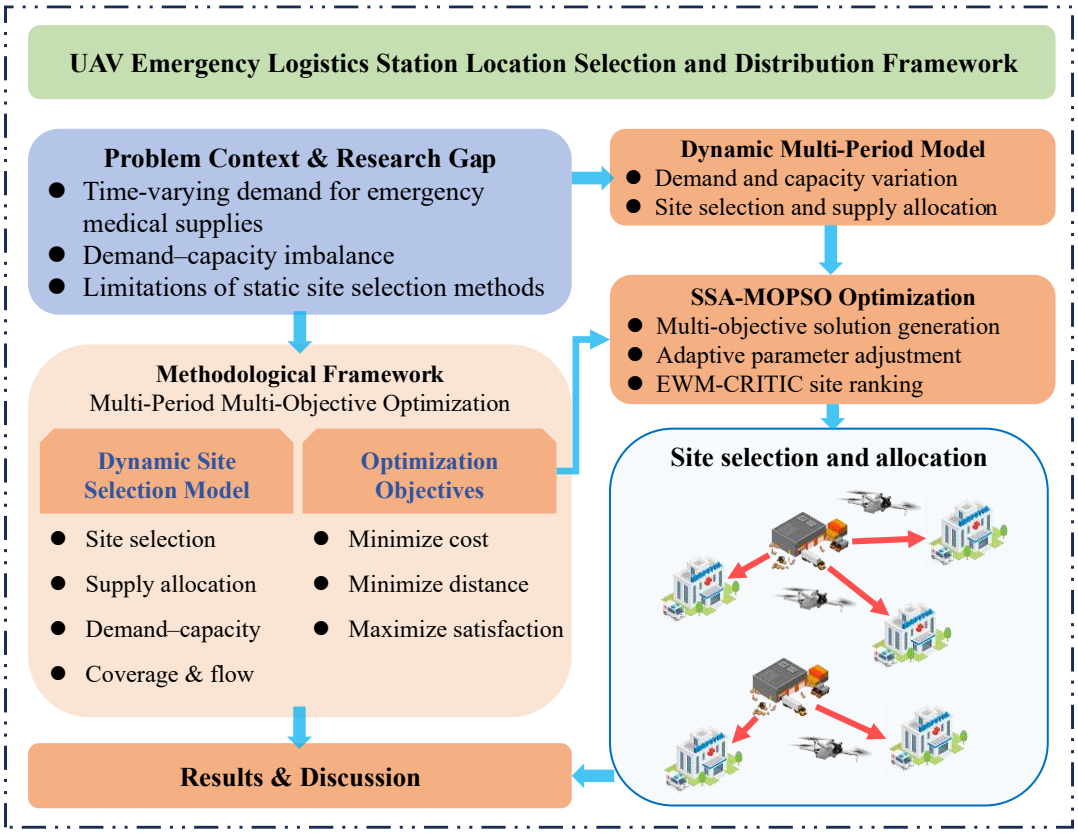


Figure 2. Schematic Diagram of Dynamic Site Selection.

3.2 Research Gap and Research Process

The proposed model formulates the dynamic emergency logistics location problem using three competing objectives: total cost, total distribution distance, and comprehensive satisfaction. These objectives are retained independently to capture trade-offs among economic efficiency, distribution efficiency, and service performance. The first objective minimizes total emergency medical supply distribution costs, comprising fixed cooperation costs for selected distribution centers, transportation costs between distribution centers and demand points, and dispatch costs associated with different categories of emergency medical supplies. Accordingly, the total cost objective is formulated as follows:

$$\begin{aligned} minF_1 = &\sum_{i\in N}\sum_{j\in M}\sum_{t\in T} a_{ij}^t Z_{ij}^t + \sum_{i\in N}\sum_{j\in M}\sum_{t\in T} d_{ij} b_{ij}^t h_{ij}^t Z_{ij}^t \\ &+ \sum_{i\in N}\sum_{j\in M}\sum_{k\in K}\sum_{t\in T} c_{ijk}^t \omega_{ijk}^t A_{ijk}^t \end{aligned} \tag{1}$$

Where a_{ij}^t represents the fixed cooperation cost of the dispatch point during period t. d_{ij} represents the distance between the demand point i and the emergency medical supplies distribution center j. b_{ij}^t represents the unit transportation cost during period t. c_{ijk}^t represents the unit dispatch cost for emergency medical supplies of category k during period t. h_{ij}^t Indicates whether, during period t, candidate point j is selected as an emergency medical supplies distribution center; if so, the value is 1; otherwise, it is 0. ω_{ijk}^t indicates the demand for emergency medical supplies of type k at demand point i during period t. Z_{ij}^t indicates whether, during period t, distribution center j serves demand point i; if so, the value is 1; otherwise, it is 0. A_{ijk}^t indicates whether, during period t, distribution center j dispatches supplies of type k to demand point i; if so, the value is 1; otherwise, it is 0.

Subject to the capacity limit for dispatched supplies, the optimal emergency medical supply distribution center must be identified from among the centers to meet the demand of each designated hospital. The objective function is to minimize the sum of the products of each distribution center's supply quantity and distance to its respective

demand point, ensuring that supply points provide support from the nearest locations to reduce total dispatch time. The minimized total distance objective function is shown in Equation 2:

$$minF_2 = \sum_{i\in N}\sum_{j\in M}\sum_{k\in K}\sum_{t\in T}\omega_{ijk}^{t} d_{ij} Z_{ij}^{t} \tag{2}$$

The satisfaction function consists of distance satisfaction and supply capacity satisfaction. Distance satisfaction is defined as the reciprocal of the ratio of the actual distance from an emergency medical supply distribution center to a demand point to the distance upper limit. A higher ratio indicates that the actual distance is closer to the distance upper limit, resulting in lower satisfaction; conversely, when the actual distance is much smaller than the distance upper limit, satisfaction is higher. Supply capacity satisfaction is defined as the ratio of the allocable quantity met by the emergency medical supplies distribution center to its maximum allocable quantity. This reflects the utilization rate of the distribution point's supply capacity; a higher ratio indicates that the distribution point's supply capacity is being utilized more fully, resulting in higher satisfaction. The satisfaction objective function is shown in Equation 3:

$$maxF_3 = \sum_{i\in N}\sum_{j\in M}\sum_{k\in K}\sum_{t\in T}\frac{\lambda_1 \omega_{ijk}^{t} A_{ijk}^{t}}{g_{ijk}^{t}} + \sum_{i\in N}\sum_{j\in M}\sum_{t\in T}\frac{\lambda_2 d_{ij} h_{ij}^{t}}{s_{ij}} \tag{3}$$

where λ_1 represents the weight of distance satisfaction in period t , λ_2 represents the weight of supply capacity satisfaction in period t , and both satisfy $\lambda_1 + \lambda_2 = 1$. g_{ijk}^{t} represents the actual quantity of Class k supplies allocated by the distribution center j to the demand point i in period t . s_{ij} represents the service radius from the distribution center to the demand point i .

Equation 4 represents the maximum allocable capacity constraint for the emergency medical supplies distribution center j during period t :

$$\sum_{i\in N}\sum_{j\in M}\sum_{k\in K}\sum_{t\in T} g_{ijk}^{t} \le L_k \tag{4}$$

In particular, L_k represents the maximum capacity for supplies of the k type.

Equation 5 represents the scheduling quantity constraint for the distribution of emergency medical supplies k from the emergency medical supplies distribution center j to the demand points i during period t :

$$\sum_{i\in N}\sum_{j\in M}\sum_{k\in K}\sum_{t\in T}\omega_{ijk}^{t} \le \sum_{i\in N}\sum_{j\in M}\sum_{k\in K}\sum_{t\in T} g_{ijk}^{t} \tag{5}$$

Equations 6 through 8 represent the flow constraints for supplies k during the distribution process in period t :

$$\sum_{i\in N}\sum_{j\in M}\sum_{k\in K}\sum_{t\in T} A_{ijk}^{t} - \sum_{i\in N}\sum_{j\in M}\sum_{k\in K}\sum_{t\in T} A_{jik}^{t} = 0 \tag{6}$$

$$\sum_{i\in N}\sum_{j\in M}\sum_{k\in K}\sum_{t\in T} A_{ijk}^{t} = 1 \tag{7}$$

$$\sum_{i\in N} Z_{ij}^{t} = 1, \quad \forall j \in M, \forall t \in T \tag{8}$$

Equation 9 represents the constraint on the number of emergency medical supply distribution centers during period t :

$$\sum_{j\in M}\sum_{t\in T} h_j^{t} = q \quad \forall t \in T \tag{9}$$

Where q represents the upper limit on the number of distribution centers that can be constructed during the period.

Equation 10 represents the weighting that places greater emphasis on site selection and supply capacity for the period t :

$$\lambda_1^{t} + \lambda_2^{t} = 1 \tag{10}$$

Equation 11 represents the range within which demand points can be served by emergency medical supply distribution centers:

$$d_{ij} \le s_{ij} \quad \forall i \in N, \forall j \in M \tag{11}$$

Equation 12 ensures that every demand point is allocated to a distribution center:

$$Z_{ij}^{t} \le h_j^{t}, \quad \forall i \in N, \forall j \in M, \forall t \in T \tag{12}$$

Equation 13 defines the 0–1 decision variables:

$$Z_{ij}^t, h_j^t, A_{ijk}^t \in \{0,1\}, \quad \forall i \in N, \forall j \in M_i, \forall k \in K, \forall t \in T \tag{13}$$

In this model, given the unique nature of public health emergencies, emergency supplies are distributed from the distribution center to demand points via drones:

$$g_{ijk}^t \geq 0 \quad \forall i \in N, j \in M, t \in T \tag{14}$$

Where g_{ijk}^t represents the quantity of emergency medical supplies of category k delivered by distribution center j to demand point i via drone.

The quantities of each type of supply received by each demand point in each period must meet its demand:

$$\sum_{j \in M} g_{ijk}^t \geq \omega_{ijk}^t \quad \forall i \in N, k \in K, t \in T \tag{15}$$

Where ω_{ijk}^t represents the demand for category k supplies at demand point i during period t .

Since all supplies are delivered via drones, the total amount of supplies provided by the distribution center j to each demand point during period t must not exceed its maximum supply capacity:

$$\sum_{i \in N} \sum_{k \in K} g_{ijk}^t \leq G_j h_j^t \quad \forall j \in M, t \in T \tag{16}$$

Where G_j represents the maximum supply capacity of distribution center j . h_j^t indicates whether distribution center j is operational during period t .

When a drone performs a delivery to the demand point i , the total weight of all types of supplies transported must not exceed the total payload capacity available for that drone flight:

$$\sum_{k \in K} \varpi_k g_{ijk}^t \leq P \rho_{ijk}^t \quad \forall i \in N, j \in M, t \in T \tag{17}$$

Where ϖ_k represents the weight of goods in category k . P represents the drone's maximum payload per flight.

ρ_{ijk}^t refers to a round-trip flight from the distribution center j to the demand point i .

The drone flies in a straight line from the distribution center j to the destination i , delivers the supplies, and then returns to the original distribution center j . The conditions for the drone to execute this delivery mission are:

$$2 d_{ij} Z_{ij}^t \leq e \quad \forall i \in N, j \in M, t \in T \tag{18}$$

Here, d_{ij} represents the distance from the distribution center j to the destination i . e represents the maximum round-trip range of the drone per flight.

CRITIC is a multi-attribute decision analysis method that determines weights by considering the correlations between indicators and the relative strengths of those indicators. Currently, the main shortcomings of CRITIC are as follows: First, CRITIC uses the formula $(1-R_{ij})$ in its calculations, where R_{ij} is the Pearson correlation coefficient between the indicators i and j . This approach does not account for the positive or negative nature of the correlation coefficient; that is, positive and negative correlations are treated as having the same numerical impact. This ignores the directionality of the correlation coefficient and may lead to a misinterpretation of the relationships between indicators. Second, although the CRITIC method considers the volatility and correlation of indicator data, it does not account for the dispersion of the indicator data. Dispersion refers to the breadth of the data distribution and can be assessed using variance, interquartile range, or other statistical measures. The dispersion of indicators is also crucial for determining weights, as indicators with high dispersion may contain more information, thereby affecting the accuracy of decision-making. The traditional CRITIC calculation steps are as follows.

Step 1: This study uses positive indicators for data standardization, followed by standardization to eliminate the effects of differing units and magnitudes across indicators:

$$X'_{ij} = \frac{X_{ij} - min\left(X_{ij}\right)}{max\left(X_j\right) - min\left(X_j\right)} \tag{19}$$

Where X_{ij} represents the raw value of the evaluation object (i) for the indicator (j). X'_{ij} represents the normalized value of the evaluation object (i) for the indicator (j).

Step 2: Calculate the Pearson correlation coefficient matrix R_{ij} for the standardized data, which reflects the linear relationships among the indicators:

$$R_{ij} = \frac{\sum_{i=1}^{n}\left(X_i - \bar{X}_j\right)\left(Y_i - \bar{Y}\right)}{\sqrt{\sum_{i-1}^{n}\left(X_i - \bar{X}\right)^2 \sum_{k=1}^{n}\left(Y_i - \bar{Y}\right)^2}} \tag{20}$$

Step 3: Determine the information content C_j by calculating volatility S_j and conflict H_j :

$$S_j = \sqrt{\frac{\sum_{i=1}^{m}\left(X_{ij} - \bar{X}_j\right)^2}{n-1}} \tag{21}$$

$$H_j = \sum_{i=1}^{n}\left(1 - R_{ij}\right) \tag{22}$$

$$C_j = S_j \times H_j \tag{23}$$

Step 4: Normalize the information content of each indicator to obtain the weight of each indicator:

$$w_j = \frac{C_j}{\sum_{j=1}^{n} C_j} \tag{24}$$

Based on the above calculation steps, the CRITIC method has the following areas for improvement and refinement: correlation coefficients can be both positive and negative. For correlation coefficients with the same absolute value, the degree of correlation between indicators should be the same. Therefore, when reflecting the comparative strength between indicators, we replace the original method's $\left(1 - R_{ij}\right)$ with $\left(1 - \left|R_{ij}\right|\right)$, resulting in $R_{ij} \in [0,1]$. The improved method is shown in Equation 30.

$$H_j = \sum_{i=1}^{n}\left(1 - \left|R_{ij}\right|\right) \tag{25}$$

Although the CRITIC method can effectively account for the correlation (conflict) and comparative intensity (volatility) among indicator data, it does not consider the degree of dispersion among the indicator data. Therefore, the CRITIC method is improved using the EWM method so that the improved CRITIC method can fully account for the inherent dispersion of the indicator data. The specific improvement method is shown in Equation31.

$$w_j = \frac{EWM_j \sum_{j=1}^{n} C_j + C_j \sum_{j=1}^{n} EWM_j}{2\sum_{j=1}^{n} EWM_j \sum_{j=1}^{n} C_j} \tag{26}$$

3.3 Algorithm Design

In light of the characteristics of the aforementioned multi-period dynamic site selection model, and to enhance the algorithm's convergence and diversity, this paper designs the SSA-MOPSO algorithm. Its core concept is as follows: First, based on the fitness of the Sparrow Search Algorithm (SSA), the crossover probability, mutation probability, and inertia weight hyperparameters of the MOPSO algorithm are dynamically updated at each iteration to avoid getting stuck in local optima and to improve solution diversity.Second, based on the multi-cycle characteristics, the demand and allocable capacity data for the next cycle ($t+1$) are updated according to the output of the current cycle (t). Finally, the optimal site selection, scheduling, and allocation plan is determined based on the set of output solutions[20,22].

The hyperparameter settings of MOPSO employ an adaptive adjustment strategy, dynamically adjusting MOPSO hyperparameters such as particle velocity and the weights of local and global optimal solutions—based on the adaptive capabilities of the Sparrow Search Algorithm (SSA) to accommodate the requirements of different cycles. The algorithm improvement steps are as follows.

Step 1: Initialize the population and SSA-related parameters. Use the current quality of the non-dominant solution set of MOPSO (measured by the composite index of HV and Spacing) as the fitness function for SSA. Every 10 generations, invoke SSA to search for the optimal parameter combination within the hyperparameter search space. Define the search spaces for the three MOPSO hyperparameters as $\left(\varpi, \eta_1, \eta_2\right)$, and calculate the fitness values of the initial population. The SSA fitness function is shown in Equation 32.

$$Q(\theta)=\frac{\beta_1}{HV(\theta)+\varepsilon}+\beta_2 Spacing(\theta) \tag{27}$$

Here, β_1 and β_2 represent the cost and satisfaction weights, respectively. θ denotes the set of non-dominant solutions in the current external archive. ε is a small constant used to prevent the denominator from becoming zero.

Step 2: Update the finder's position $W_{ij}^{\ell+1}$.

$$W_{ij}^{\ell+1}=\begin{cases} W_{ij}^{\ell}\cdot exp\left(-\dfrac{i}{\alpha\cdot iter_{max}}\right) & if \quad R_2<ST \\ W_{i,j}^{\ell}+O\cdot P & if \quad R_2\geq ST \end{cases} \tag{28}$$

Here, t represents the current iteration number. $iter_{\max}$ is a constant representing the maximum number of iterations. W_{ij} represents the position of the i sparrow in the j dimension. $\alpha\in(0,1]$ represents a random number. $R_2\left(R_2\in[0,1]\right)$ and $ST\left(ST\in[0.5,1]\right)$ represent the early warning value and safety value, respectively. O is a random number following a normal distribution. P represents the matrix $1\times n$, where all elements are 1.

Step 3: Update the subscriber's position W_{ij}^{t+1}.

$$W_{ij}^{\ell+1}=\begin{cases} O\cdot exq\left(\dfrac{W_{worst}-W_{ij}^{\ell}}{i^2}\right) & if \quad i>n/2 \\ W_p^{\ell+1}+\left|W_{ij}^{\ell}-W_p^{\ell+1}\right|\cdot B^{+}\cdot L & otherwise \end{cases} \tag{29}$$

Here, W_p is the optimal position currently occupied by the discoverer, while W_{worst} represents the current globally worst position. B denotes a $1\times n$ matrix whose elements are randomly assigned values of 1 or -1, and $B^{+}=B^{T}(BB^{T})^{-1}$. When $i>n/2$, this indicates that the i joiner with the lowest fitness has not obtained food and is in a state of extreme hunger; at this point, it needs to fly elsewhere to forage for more energy.

Step 4: Update the positions of the sparrows that have become aware of the danger: $W_{ij}^{\ell+1}$.

$$W_{ij}^{\ell+1}=\begin{cases} W_{best}^{\ell}+\varphi\cdot\left|W_{ij}^{\ell}-W_{best}^{\ell}\right| & if \quad Q_i>Q_{\max} \\ W_{ij}^{\ell}+G\cdot\left(\dfrac{\left|W_{ij}^{\ell}-W_{worst}^{\ell}\right|}{(Q_i-Q_{\min})+\varepsilon}\right) & if \quad Q_i=Q_{\max} \end{cases} \tag{30}$$

Here, φ represents a random number following a normal distribution with a mean of 0 and a variance of 1. ε is a very small constant that prevents the denominator from becoming zero.

By using SSA to search for the optimal hyperparameter solution in the (ϖ,η_1,η_2) space—minimizing the fitness function Q —the MOPSO algorithm avoids converging to local optima, ensuring the rationality of site selection.

The MOPSO algorithm uses the concept of Pareto dominance to determine the flight direction of particles. By comparing dominance relationships among particles, non-dominated individuals are identified and stored in the global elite pool. Based on the density-adaptive mesh estimation method, the globally optimal solution G_{best} is selected from the global elite pool,simultaneously, by comparing dominance relationships among individuals across new and old generations, the historical optimal solutions are selected P_{best}. The velocities and positions of the particles are continuously updated using Equation (36), ultimately yielding a set of non-dominant solutions that cover the entire search space, are uniformly distributed, and lie close to the Pareto front, all with minimal computational resources.

$$x_i^{\ell+1}=x_i^{\ell}+v_i^{\ell+1} \tag{31}$$

In the equation, x_i represents the value of the solution vector in the i dimension; ℓ represents the number of iterations; and v_i represents the velocity component of a particle in the direction of the i dimension.

To enhance the MOPSO algorithm's ability to escape local optima, this study proposes an elite backward learning method to prevent particles from clustering at the boundary and wasting search resources. In each generation, a number of elites with the largest crowding distance from the external archive are selected, and their backward solutions are generated:

$$x_i^{*}=lb+ub-x_i \tag{32}$$

Where, if $x_i^* < x_i$, the replacement $x_i \leftarrow x_i^*$ is performed. lb and ub represent the lower and upper bound vectors of the search space, respectively.

Let the j component of a particle's position be $x_j \in [0,1]$; after the update, its position becomes x_j' . The boundary rebound formula is:

$$x_j'' = \begin{cases} -x_j', & x_j' < 0 \\ 2 - x_j', & x_j' > 1 \\ x_j', & otherwise \end{cases} \tag{33}$$

Where x_j' represents the j component after the velocity update, and x_j'' represents the component after boundary bounce processing. The velocity update is calculated as follows:

$$v_i^{\ell+1} = \varpi v_i^{\ell} + \eta_1 r_1 \left(P_{i,best}^{\ell} - x_i^{\ell} \right) + \eta_2 r_2 \left(G_{best}^{\ell} - x_i^{\ell} \right) \tag{34}$$

In this equation, $P_{i,best}^{\ell}$ represents the individual's historical optimal position for the i particle up to the ℓ th iteration. ϖ represents the inertial weight. η_1 represents the individual learning factor. η_2 represents the social learning factor. G_{best}^{ℓ} represents the global guide position selected from the current external elite population.

The density-adaptive grid estimation method is used to select the globally optimal solution from the global elite pool (REP) and to prune particles on the Pareto front. Particle density estimates are obtained by dividing the objective function space into equal-sized grids and counting the number of particles in each grid. The fewer particles in a grid, the lower its density value; conversely, the more particles, the higher the density value. The algorithm steps are as follows.

Step 1: Partition the objective space, determine the upper and lower bounds $\left(\min F_i^{\ell}, \max F_i^{\ell} \right)$ for each dimension of the objective space, and calculate the modulus of the grid.

$$\Delta F_i^{\ell} = \frac{\max F_i^{\ell} - \min F_i^{\ell}}{M} \tag{35}$$

Where F_i^{ℓ} is the objective function value for the i dimension, $i = 1, 2, \cdots, n$; and M is the number of grids to be partitioned for the i th dimension.

Step 2: Iterate through the particles in the external archive and calculate the grid number in which each particle is located.

Step 3: Determine the probability that a particle is located in a given grid based on its ID.

$$r_k = \frac{1}{Num_k} \tag{36}$$

Where Num_k represents the number of particles in the k grid.

Step 4: As shown in Figure 3, introduce random perturbations via the mutation operator to prevent the particle swarm from getting stuck in local optima and to enhance the algorithm's global search capability.

Step 5: Generate random numbers to select particles within the grid. The grid partitioning method is used to determine the prey's position, thereby preventing the algorithm from getting stuck in local optima. Additionally, to improve the algorithm's convergence speed, when the population exceeds the boundaries, the algorithm does not directly assign boundary values to individuals; instead, it assigns the corresponding values beyond the boundaries to the prey's position, thereby avoiding repeated searches of boundary locations.

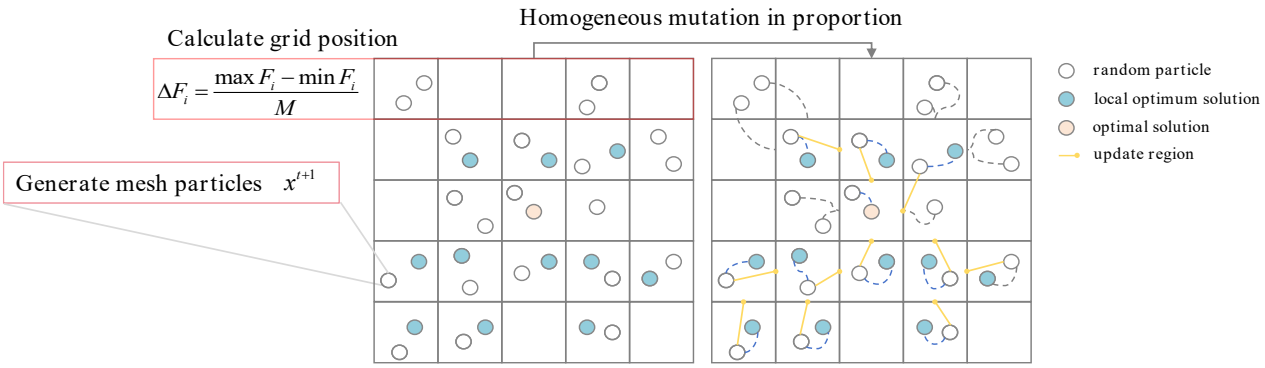


Figure 2. Schematic diagram of particle update and mutation strategies.

As shown in Table1, SSA-MOPSO first randomly generates particle positions and velocities within a specified range, and calculates the cost, distribution distance, and satisfaction level of each particle based on

the site selection model, saving the initial non-dominated solutions to an external archive. In each iteration, a leading particle is selected from the sparse grid of the archive, and the particle velocity and position are updated by incorporating inertia weight, individual learning factor, and social learning factor, with the search process further refined through velocity limiting, position truncation, and random mutation. Upon reaching a preset adjustment cycle, SSA is employed to search for new parameter combinations within given parameter ranges, using the quality metrics of the solution set as evaluation criteria, and updates the inertia weight and the two learning factors of MOPSO. After completing particle evaluation, the algorithm updates individual optimal solutions and the external archive based on the Pareto dominance relationship, while removing dominated and duplicate solutions, and controls the archive size using grid density. Subsequently, elite solutions are selected from the sparse grid to generate opposition-based solutions; such opposition-based solutions are used to replace the original elite solutions only when they dominate the latter. At the end of the iterations, the Pareto solution set is output, and the cost, distance, satisfaction, and parameter variations for each cycle are recorded.

Algorithm 1 SSA-MOPSO algorithm	
Input: Emergency logistics model M, MOPSO parameters, SSA parameters, and random seed s.	
Output: Pareto archive.	
1:	Initialize $X_{ij} \in U(0,1)$ and $V_{ij} \in (-v_{max}, v_{max})$;
2:	Evaluate $F_i = (f_1, f_2, f_3)$, where
3:	**Set** $P_{best}(X) = X_i$ and $P_{best}(F_i) = F(X_i)$, **then** update archive A;
4:	**for** $t = 0,1,\ldots,T-1$ **do**
5:	**if** $t > 0$ and t mod $Delta = 0$ **then**
6:	Generate SSA individuals $z_k = (w_k, c_{1k}, c_{2k})$ within their bounds;
7:	Evaluate each parameter combination using
8:	$Q_k = \beta_s S(F) / (\beta_h H(F) + \varepsilon)$
9:	Sort the individuals and update discoverers, joiners, and danger-aware agents;
10:	Apply parameter bounds and recalculate Q_k
11:	Select the individual with the minimum Q and update (w_k, c_{1k}, c_{2k})
12:	**end if**
13:	Select a leader L_i from a sparse grid in the external archive;
14:	Update velocity: $V_i \leftarrow wV_i + c_1 r_1 (P_{best}(X_i) - X_i) + c_2 r_2 (L_i - X_i)$
15:	Limit velocity: $V_i \leftarrow clip(V_i, -v_{max}, v_{max})$
16:	Update position: $X_i \leftarrow clip(X_i + V_i, 0, 1)$
17:	With probability r_m, reset a randomly selected component: $X_i < -U(0,1)$
18:	Evaluate F_i and update the personal best according to Pareto dominance;
19:	Merge the current solutions with A and remove dominated and duplicate solutions;
20:	Remove solutions from crowded grids until $\lvert A \rvert \le A_{max}$;
21:	Generate an elite opposite solution $X^{opp} = 1 - X_e$ and retain the better solution;
22:	Record $\lvert A \rvert$, cost, distance, satisfaction, and the current parameter values;
23:	**end for**
24:	**Return** Pareto archive A_X and A_F

Table 1. SSA-MOPSO code.

3.4 Stock and flow diagram formulation

The empirical analysis uses data on available beds, bed demand, and medical-supply allocation for 48 desig-nated hospitals in Wuhan, covering 12-25 February 2020. The observation window captures substantial temporal variation in both demand intensity and supply allocation, providing an appropriate basis for evaluating the pro-posed multi-period location framework. Figure 4 summarizes the principal characteristics of the dataset used in the optimization experiments.

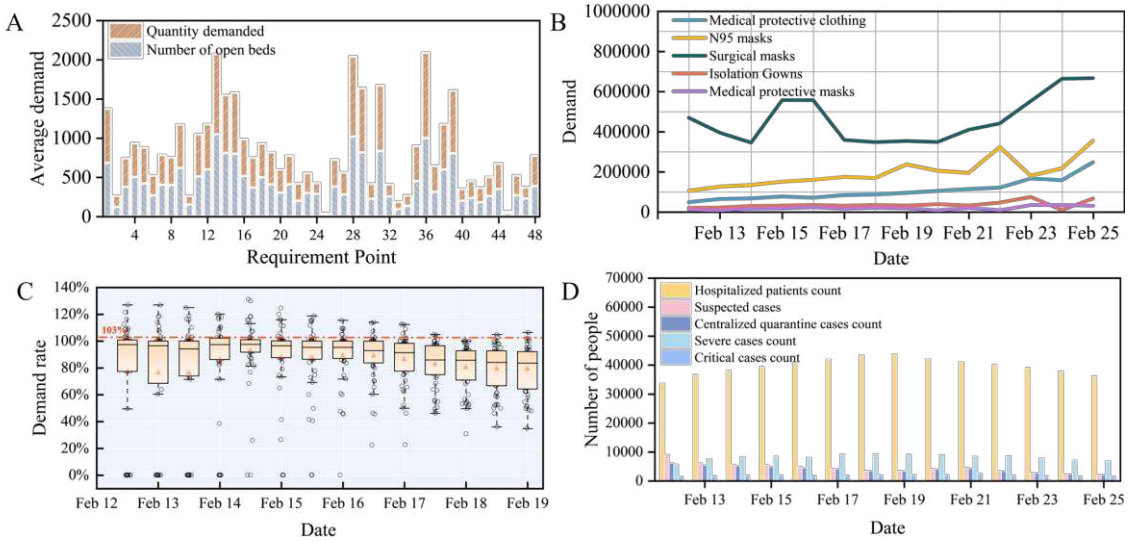


Figure 4. Data Characteristics Analysis.

Ethics Statement: this study did not involve human participants, human tissue, clinical interventions, or individual-level patient or medical-record data. The empirical analysis was based exclusively on aggregated hospital-level operational data, including available beds, bed demand, medical-supply allocation, and facility characteristics of designated hospitals in Wuhan. No personally identifiable information or individual-level health information was collected, accessed, or analyzed. Accordingly, institutional ethics approval and informed consent were not applicable to this study.

4 Experiment

4.1 Parameter Calibration

Computational experiments were conducted on a server equipped with a 16-core Intel Xeon Platinum 8352V processor (2.10 GHz), 62 GB RAM, and two NVIDIA GeForce RTX 4080 GPUs (32 GB each). To reflect changing priorities across emergency stages, the SSA fitness-function weights for Cycles 1–3 were set to (0.3, 0.7), (0.5, 0.5), and (0.6, 0.4), respectively [23-26]. Transportation and cooperation costs were specified as CNY 6–8/km and CNY 800–2,000, respectively, while the dispatch-cost parameter for medical protective suits was 100–120 suits per CNY. As reported in Table 1, MOPSO and SSA both used a population size of 300 and 200 iterations. MOPSO parameters were bounded at 0.3–0.9 for inertia weight and 1.5–2.5 for both learning factors. SSA used an early-warning threshold of 0.8, with discoverer and joiner proportions of 0.2 and 0.8, respectively.

Model	Parameter	Description	Set Value
MOPSO	Number of Particles	Coverage of the search space	300
	Number of Iterations	Algorithm termination threshold	200
	Inertia Weight	Control particle velocity	(0.3, 0.9)
	Individual learning factor	Controls the particle's movement toward the local historical best position	(1.5, 2.5)
	Social learning factor	Controls particles to move toward the global optimal position	(1.5, 2.5)
SSA	Number of Iterations	Algorithm termination threshold	200
	Population Size	Number of sparrows	300

	Early warning threshold	Threshold for determining whether a natural predator threat exists	0.8
	Proportion of Detections	Exploration of new solution spaces	0.2
	Proportion of joiners	Position Update	0.8

Table 2. Algorithm parameter settings.

4.2 Model Solution

The four algorithms exhibited clear convergence over 200 iterations (Figure 5). Total cost and distribution distance declined rapidly before stabilizing after approximately 100 iterations, whereas comprehensive satisfaction increased and stabilized after approximately 50 iterations. SSA-MOPSO achieved lower final cost and distance while maintaining higher satisfaction. Compared with conventional MOPSO, it reduced distribution distance by 10,406.195 km and total cost by CNY 72,843.371, while increasing comprehensive satisfaction by 0.689%. These results indicate that SSA-based adaptive parameter adjustment improves MOPSO search performance and provides a more favorable balance among the three competing objectives under the experimental conditions.

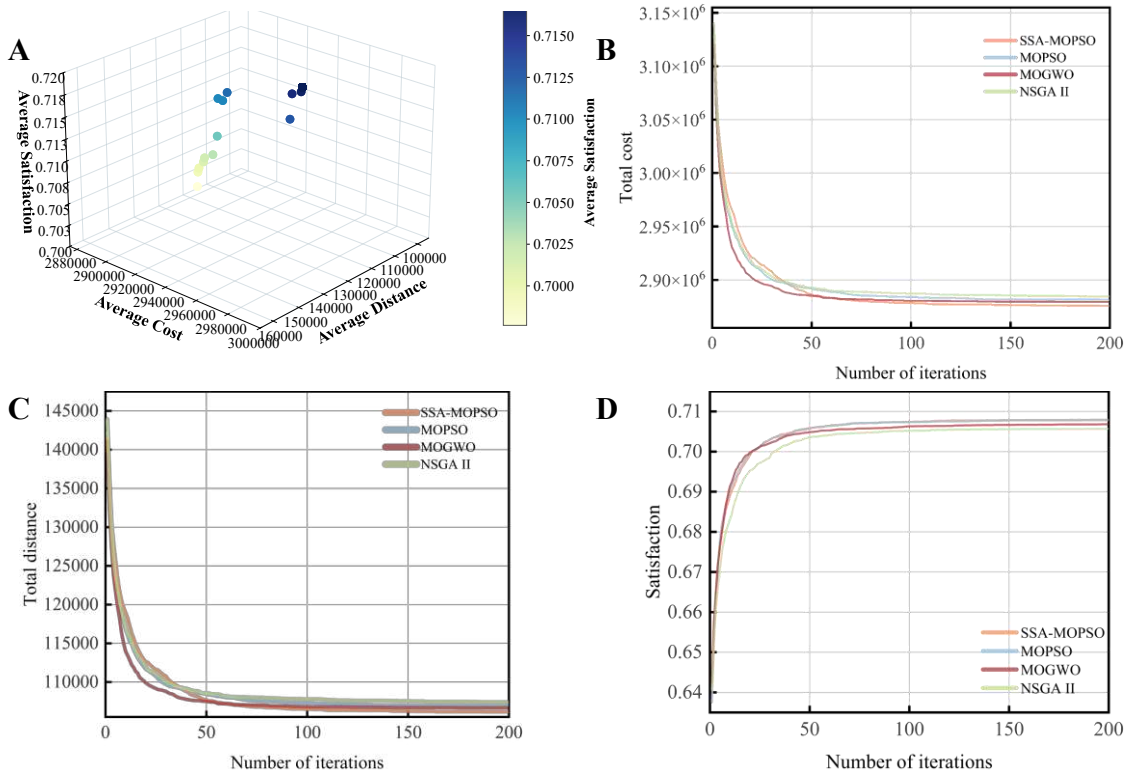


Figure 5. Set of Pareto solutions.

Across all three cycles, total distribution distance decreased as the number of selected distribution centers increased, as additional facilities enabled demand points to be assigned to closer locations. However, this relationship varied across cycles. Cycle 1 exhibited shorter total distances because lower demand allowed greater emphasis on spatial proximity. As demand increased in Cycles 2 and 3, distribution-center capacity became more influential in site selection. Candidate facilities therefore had to satisfy both proximity and capacity requirements, limiting the ability to prioritize distance alone. Consequently, the higher capacity requirements in later cycles resulted in comparatively greater total distribution distances[27-29].

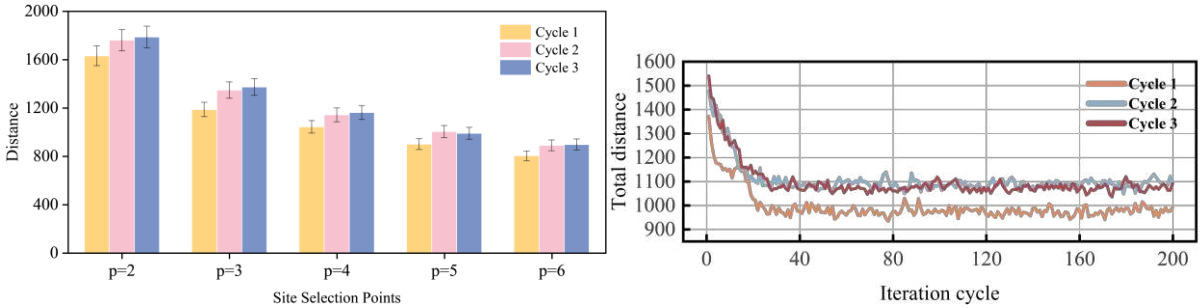


Figure 6. Relationship Between the Number of Locations and Total Distance.

The cycle-specific results in Table 3 confirm the dynamic nature of site selection. During the initial stage, temporary distribution centers can be located near designated hospitals to respond efficiently to concentrated demand. As demand increases in Cycles 2 and 3, however, capacity constraints become more influential, and facilities adequate under lower demand may no longer satisfy emerging requirements. Accordingly, the number and combination of active distribution centers should be adjusted across cycles. The multi-period model enables additional facilities to be activated when existing capacity becomes insufficient while accounting for candidate-site capacity and operating conditions. These findings support treating emergency logistics site selection as a dynamic location-allocation problem rather than a static, one-time decision.

Importantly, Table II also illustrates that a site with a high level of satisfaction is not necessarily the preferred facility in every cycle. Site-selection decisions emerge from the simultaneous consideration of demand coverage, satisfaction, cost, and capacity conditions. The results therefore reflect the trade-offs embedded in the multi-objective formulation rather than optimization with respect to any single performance measure.

Cycle	Site	Total Demand Covered	Overall Satisfaction	Total Cost (10,000 yuan)
T=1	Huoshenshan Hospital	9,658	0.72	106.28
	Wuhan Third Hospital	17,385	0.68	191.28
	Wuhan Ninth Hospital	19,317	0.69	212.53
	Wuhan Red Cross Hospital	28,975	0.84	318.77
	Wuhan Traditional Chinese Medicine Hospital	17,385	0.88	191.28
T=2	Huoshenshan Hospital	26,558	0.71	292.18
	Wuhan Third Hospital	29,508	0.76	324.63
	Wuhan Sixth Hospital	44,263	0.69	486.94
	Wuhan Traditional Chinese Medicine Hospital	26,558	0.78	292.18
	Huangpi District Hospital of Traditional Chinese Medicine	14,754	0.72	162.34
T=3	Tongji Sino-French New Town Campus	27,714	0.69	304.90
	Wuhan Third Hospital	69,286	0.72	762.19
	Wuhan Ninth Hospital	55,429	0.70	609.76
	Wuhan Red Cross Hospital	138,572	0.81	1,524.34
	Wuhan Traditional Chinese Medicine Hospital	41,572	0.78	457.34

Table 3. Site selection decision schemes for different cycles.

4.3 Evaluation Analysis

The optimization identifies candidate distribution centers across emergency cycles, but their activation sequence must also reflect medical-material storage requirements. Emergency medications and antibiotics require controlled temperature and humidity conditions; therefore, closing or relocating an activated facility may disrupt storage continuity and subsequent allocation. Candidate sites were consequently evaluated using the proposed EWM-CRITIC procedure. As reported in Table 4, the evaluation integrates facility characteristics and optimization outcomes, including number of beds, total floor area, site area, hospital grade, total demand covered, overall satisfaction, and total dispatch cost. Demand, satisfaction, and cost were derived from cycle-specific optimization results, whereas facility characteristics were obtained from the relevant official websites.

Objective weighting is well suited to dynamic emergency logistics because changing medical-supply demand can alter both indicator values and candidate-site performance. Unlike subjective approaches requiring repeated expert assessment, objective weighting enables rankings to be recalculated directly from updated data. As shown in Table 5, the EWM-CRITIC evaluation ranked Wuhan Red Cross Hospital first (0.165), followed by Wuhan Traditional Chinese Medicine Hospital (0.138) and Tongji Sino-French New Town Campus (0.134). Wuhan Third Hospital (0.127), Huoshenshan Hospital (0.115), Huangpi District Hospital of Traditional Chinese Medicine (0.113), Wuhan No. 9 Hospital (0.105), and Wuhan Sixth Hospital (0.103) occupied the remaining positions.

Site Location	Number of Beds	Total Floor Area (10,000 square meters)	Site Area (square meters)	Hospital Grade	Total Demand Covered (units)	Overall Satisfaction	Total Dispatch Cost (10,000 yuan)
Huoshenshan Hospital	1,000	3.39	50,000	3	18,108	0.72	199.23
Wuhan Third Hospital	1,900	4.73	146,838	3	38,726	0.72	426.03
Wuhan Sixth Hospital	500	5.26	30,000	3	44,263	0.69	486.94
Wuhan No. 9 Hospital	600	3.20	23,000	2	37,373	0.70	411.15
Wuhan Traditional Chinese Medicine Hospital	1,088	2.80	7,000	3	28,505	0.81	313.60
Wuhan Red Cross Hospital	500	2.31	10,420	2	83,774	0.83	921.56
Huangpi District Hospital of Traditional Chinese Medicine	1,088	2.88	40,000	2	14,754	0.72	162.34
Tongji Sino-French New	1,000	15.00	123333	3	27,714	0.69	304.90

Town Campus							

Table 4. Comprehensive evaluation indicators.

Site	Information Entropy Value	Coefficient of Variation	Volatility	Conflict	Information Content	Composite Weight	Rank
Huoshenshan Hospital (TJH-SFNCC)	0.342	0.658	0.378	1.835	0.694	0.115	5
Wuhan Third Hospital (HPDHTCM)	0.298	0.702	0.373	2.156	0.805	0.127	4
Wuhan Sixth Hospital (WRCH)	0.383	0.617	0.418	1.407	0.588	0.103	8
Wuhan No. 9 Hospital (WHTCM)	0.385	0.615	0.407	1.513	0.616	0.105	7
Wuhan Traditional Chinese Medicine Hospital (WNH)	0.340	0.660	0.370	2.684	0.994	0.138	2
Wuhan Red Cross Hospital (WSH)	0.221	0.779	0.372	3.233	1.202	0.165	1
Huangpi District Hospital of Traditional Chinese Medicine (WTH)	0.353	0.647	0.378	1.819	0.687	0.113	6
Tongji Sino-French New Town Campus (HSSH)	0.271	0.729	0.372	2.299	0.856	0.134	3

Table 4. EWM-CRITIC comprehensive evaluation results.

The ranking directly informs the dynamic activation strategy, particularly when initial emergency demand is difficult to predict. Within the proposed framework, Wuhan Red Cross Hospital, as the highest-ranked candidate, was selected as the initial distribution center. Additional facilities were subsequently activated according to evolving demand, available storage capacity, and medical-material storage requirements. Thus, comprehensive evaluation translates cycle-specific optimization results into a sequential activation strategy. As shown in Figure 7, EWM generates relatively balanced weights, whereas CRITIC emphasizes indicator variability and independence. EWM-CRITIC integrates these complementary information structures, providing the combined weighting mechanism for final site ranking within the dynamic site-selection framework.

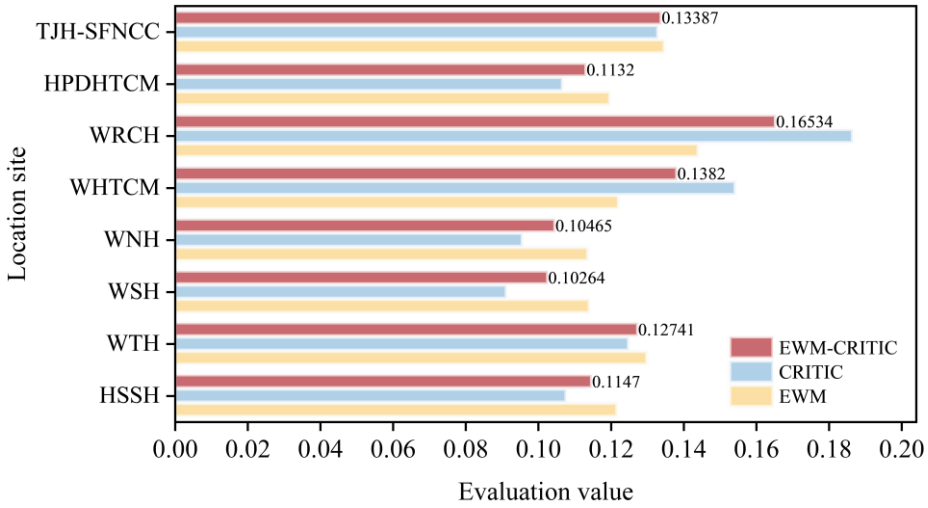


Figure 7. Comprehensive Weights.

4.4 Model Comparison Experiment

To evaluate SSA-MOPSO, its performance was compared with NSGA-II, MOGWO, and conventional MOPSO using Hypervolume (HV), Spacing, the number of non-dominated solutions, and computational time. Spacing measures the distribution uniformity of non-dominated solutions, with lower values indicating greater uniformity, whereas HV quantifies the dominated objective-space volume relative to a reference point, with higher values indicating broader coverage and stronger overall performance. During optimization, SSA-MOPSO initially exhibited fluctuations in Spacing, which declined rapidly and stabilized at a comparatively low level after approximately 50 iterations. In contrast, the benchmark algorithms showed greater fluctuations or higher Spacing values during the middle and later iterations. These results indicate that SSA-MOPSO achieves greater late-stage solution-distribution stability under the experimental configuration.

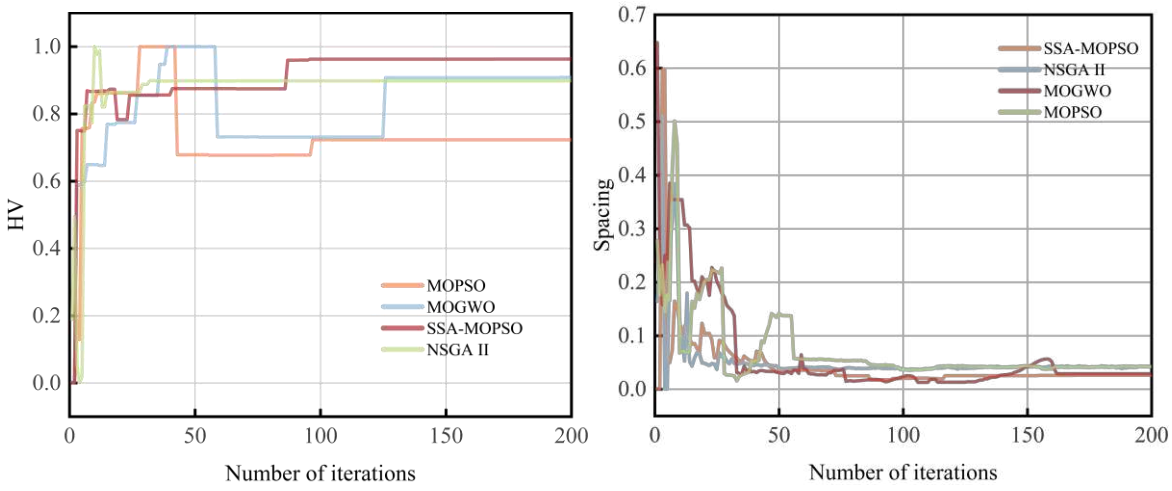


Figure 8. Comparison of Hypervolume (HV) and Spacing Iterations.

The quantitative comparison further confirms the performance differences. SSA-MOPSO achieved the highest HV (8,290,050,000), exceeding NSGA-II, MOGWO, and MOPSO by 13.67%, 7.38%, and 4.85%, respectively. It also produced the lowest Spacing (0.02553), representing reductions of 39.36%, 10.58%, and 38.84%, respectively, and indicating greater

solution-distribution uniformity. Computationally, SSA-MOPSO generated 15 non-dominated solutions in 327 s, compared with seven in 344 s for NSGA-II, 11 in 378 s for MOGWO, and eight in 343 s for MOPSO. Thus, SSA-MOPSO achieved the largest non-dominated solution set and shortest computational time under the experimental setting.

Model	HV	Spacing	Number of Solutions	Training Time (s)
NSGA II	0.89787	0.0421	7	344
MOGWO	0.90819	0.02855	11	378
MOPSO	0.72246	0.04174	8	343
SSA-MOPSO	0.9628	0.02553	15	327

Table 6. Final performance comparison.

The spatial configurations further differentiate algorithm performance. NSGA-II and MOPSO produce comparatively dispersed solutions, characterized by longer distribution paths and partial overlap among facility service areas, while MOGWO yields a more concentrated configuration but retains several distant demand assignments. In contrast, SSA-MOPSO positions selected facilities closer to concentrated demand areas and generates a more compact distribution network while maintaining demand coverage. These spatial patterns are consistent with the HV and Spacing results, indicating that the adaptive parameter mechanism improves location-allocation quality under the experimental conditions.

Overall, the experimental results consistently support SSA-MOPSO. The algorithm achieves favorable cost, distance, and satisfaction outcomes, while HV and Spacing indicate stronger Pareto-set coverage and distribution uniformity than the benchmark algorithms. Its spatial configuration also provides a more compact relationship between distribution centers and demand points. Collectively, these findings demonstrate the effectiveness of SSA-MOPSO for the multi-period dynamic emergency logistics site-selection problem under the evaluated experimental conditions.

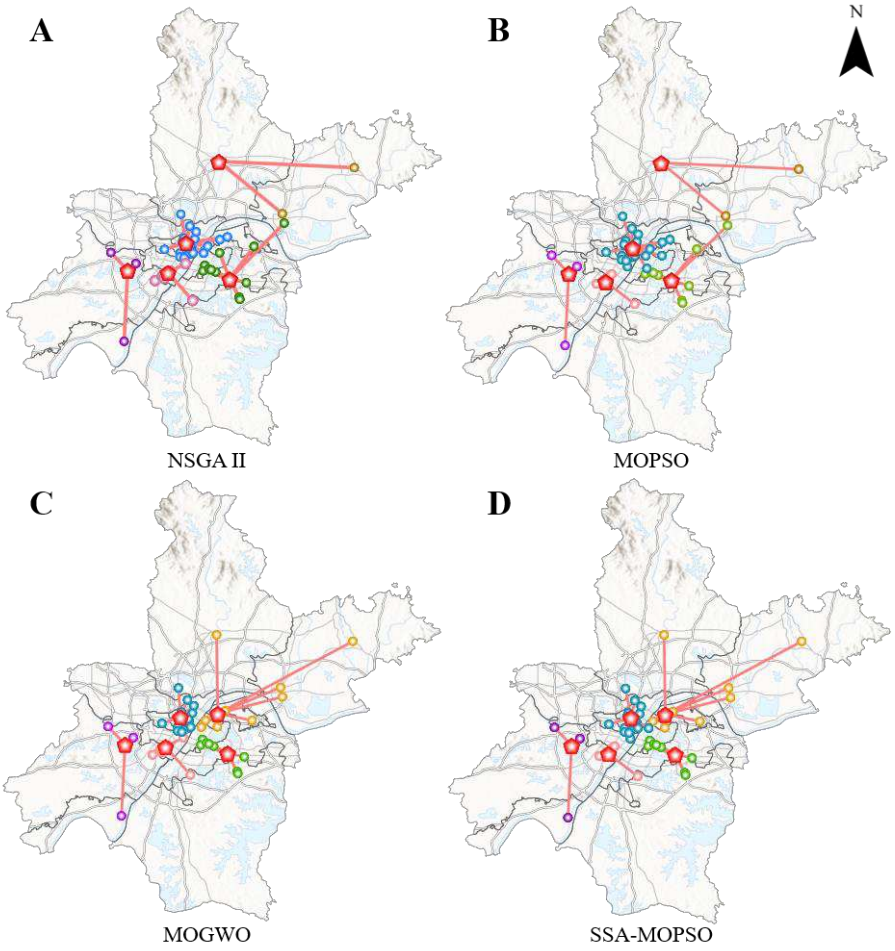


Figure 8. Comparison of Site Selection Schemes from Different Algorithms.

5. CONCLUSION

This study presents a multi-period, multi-objective framework for dynamic emergency medical logistics site selection, minimizing cost and distance while maximizing satisfaction. It integrates SSA with MOPSO (SSA-MOPSO) featuring adaptive parameter tuning, and uses EWM-CRITIC to prioritize candidate centers. A Wuhan case validates the framework under changing demand and capacity.

The findings first confirm the importance of treating emergency facility location as a dynamic rather than static decision. During periods of relatively low demand, spatial proximity exerts greater influence on facility selection because available capacity is generally sufficient to satisfy demand. As demand increases, however, facility capacity and demand coverage become increasingly restrictive. Consequently, neither the number of active distribution centers nor the associated allocation scheme should remain fixed throughout an emergency. Instead, network configurations should evolve according to period-specific demand and capacity conditions.

Second, the results demonstrate the effectiveness of SSA-based adaptive parameter adjustment within MOPSO. By dynamically regulating the inertia weight and individual and social learning factors, SSA-MOPSO improves the balance between global exploration and exploitation of high-quality solutions. Compared with conventional MOPSO, the proposed algorithm reduces total distribution distance by 10,406.195 km and total cost by CNY 72,843.371, while increasing comprehensive satisfaction by 0.689%. The resulting solutions also exhibit a more compact spatial configuration and improved distribution of non-dominated alternatives.

Third, EWM-CRITIC provides an objective mechanism for translating multi-period optimization outcomes into an operational facility-activation sequence. Wuhan Red Cross Hospital achieves the highest comprehensive weight (0.165) and is therefore identified as the preferred initial site, followed by Wuhan Traditional Chinese Medicine Hospital and Tongji Sino-French New Town Campus. Additional facilities can subsequently be activated as demand, storage capacity, and medical-material storage requirements evolve. This sequential mechanism links mathematical optimization with practical implementation while preserving operational continuity across emergency periods.SSA-MOPSO outperforms NSGA-II, MOGWO, and MOPSO with the highest Hypervolume and lowest Spacing of 0.02553, consistent with its compact facility-demand allocation and demand coverage.Operationally, emergency networks should not rely solely on fixed facilities. Candidate sites can be pre-evaluated and activated sequentially as demand changes. Multi-period optimization with objective prioritization balances distance, capacity, cost, and satisfaction, and guides both location and activation timing.

These findings are bounded by Wuhan COVID-19 data and exclude congestion, vehicle configurations, time windows, and demand forecast errors. Future research may add real-time traffic, dynamic forecasting, and multi-supply coordination, broadening practical applicability while keeping the dynamic multi-period multi-objective structure.

Data availability

The datasets used and/or analyzed during the current study are available from the corresponding author on reasonable request.

References

1. Wang, F. Y., Tang, T., Li, Y. et al. A review of research on emergency resource supply and allocation under major sudden disasters. J. Nat. Disasters 30(4), 44–54 (2021). doi:10.13577/j.jnd.2021.0405.

2. He, S. S., Guo, Y., Zhu, W. H. et al. Bi-objective optimization of emergency logistics network considering equilibrium relaxation inventory under pandemic. Railw. Transp. Econ. 45(1), 16–22, 29 (2023). doi:10.16668/j.cnki.issn.1003-1421.2023.01.03.
3. Zhang, L. & Li, J. Z. Research on location-routing stochastic optimization problem of emergency disaster relief based on road reliability. J. Syst. Sci. Math. Sci. 43(10), 2480–2502 (2023).
4. Teng, H. J., Shu, Z. L., Zhang, X. et al. Research on optimization method of emergency logistics distribution system model for earthquake disasters. J. Saf. Sci. Technol. 19(4), 160–167 (2023).
5. Yang, Y., Hao, X. & Wang, S. The drone scheduling problem in shore-to-ship delivery: A time discretization-based model with an exact solving approach. Transp. Res. Part B Methodol. 191, 103117 (2025). https://doi.org/10.1016/j.trb.2024.103117
6. Hu, X. B., Yuan, L. Y., Li, H. et al. Emergency evacuation path optimization based on ripple-spreading algorithm. J. Transp. Syst. Eng. Inf. Technol. 24(1), 253–261 (2024).DOI:10.16097/j.cnki.1009-6744.2024.01.025.
7. Zhou, B., Zeng, W., Liu, W. & Yang, H. Scheduling UAV-assisted urban subway inspection services. Transp. Res. Part B Methodol. 199, 103287 (2025). https://doi.org/10.1016/j.trb.2025.103287
8. Wu, R. & He, G. X. Simulation research on dynamic location of logistics distribution centers for construction supply chain materials. Constr. Econ. 44(S2), 583–587 (2023). DOI:10.14181/j.cnki.1002-851x.2023S2583.
9. Luo, Y. & Zhang, Y. Day-ahead scheduling of wind-solar-pumped storage system based on predictive mutation multi-objective particle swarm optimization. Renew. Energy Resour. 41(11), 1484–1490 (2023). doi: 10.13941/j.cnki.21-1469/tk.2023.11.012.
10. Wang, X. P., Lu, W., Li, R. Q. et al. A literature review on metro freight based on underground logistics system. Chin. J. Undergr. Space Eng. 19(S2), 534–539, 548 (2023).
11. Li, S. F. Research on optimization of railway emergency logistics system. Railw. Transp. Econ. 43(1), 29–33 (2021). doi:10.16668/j.cnki.issn.1003-1421.2021.01.05.
12. Xue, J. & Shen, B. A novel swarm intelligence optimization approach: sparrow search algorithm. Syst. Sci. Control Eng. 8, 22–34. doi: 10.1080/21642583.2019.1708830.
13. Andres, B., Díaz-Madroñero, F. M., Soares, A. L. & Poler, R. Enabling technologies to support supply chain logistics 5.0. IEEE Access 12, 43889–43906 (2024). doi: 10.1109/ACCESS.2024.3374194.
14. Luo, L., Wan, X. Y. & Wang, Q. Y. A multi-period location–allocation model for integrated management of emergency medical supplies and infected patients during epidemics. Comput. Ind. Eng. 173, 108705 (2022). doi: 10.1016/j.cie.2022.108705.
15. Awadallah, M. A. & Al-Betar, M. A. Recent versions and applications of sparrow search algorithm. Arch. Comput. Methods Eng. 30, 2831–2858 (2023).doi: 10.1007/s11831-023-09887-z.
16. Fei, T., Wang, H., Liu, L. et al. Research on multi-strategy improved sparrow search optimization algorithm. Math. Biosci. Eng. 20, 17220–17241 (2023). doi: 10.3934/mbe.2023767.
17. Yan, X. B., Fang, Y. W. & Peng, W. S. Multi-objective Harris Hawk optimization algorithm based on adaptive Gaussian mutation. J. Beijing Univ. Aeronaut. Astronaut. 50(8), 2636–2645 (2024).doi: 10.13700/j.bh.1001-5965.2022.0686.
18. C. Chen, X. -Y. Yan, H. -R. Qi, et al., “Evaluation Method for Rooftop PV Access to Distribution Network Based on FAHP–Improved CRITIC Combined Weighting,” Power System Protection and Control, vol. 51, no. 15, pp. 97–108, 2023, doi: 10.19783/j.cnki.pspc.230072.
19. Wang, T., Zhou, H. & Tian, X. Drone scheduling optimization for shore-to-ship delivery and waste recycling. Transp. Res. Part E Logist. Transp. Rev. 209, 104708 (2026). https://doi.org/10.1016/j.tre.2026.104708
20. Meng, S., Chen, Y. & Li, D. Pickup and delivery problem with multi-visit drones considering soft time windows. Transp. Res. Part C Emerg. Technol. 180, 105359 (2025). https://doi.org/10.1016/j.trc.2025.105359
21. Du, B., Tang, A., Ye, H., Yue, H., Xu, C., Hao, L., He, H. & Liao, X. Collaborative vehicle-mounted multi-UAV routing and scheduling optimization for remote sensing observations. Drones 9, 783 (2025). https://doi.org/10.3390/drones9110783
22. Zhou, S., Han, S., Yang, M. & Du, B. A hybrid differential evolution algorithm for distributed assembly flexible job shop scheduling with batch delivery and inventory. Sci. Rep. 16, 4280 (2026). doi: 10.1038/s41598-025-34395-4
23. Zhang, P., Zhang, C., Zhang, P., Yan, X. & Yang, H. Optimization of emergency logistics for urban flooding with consideration of rainfall effects. Sci. Rep. 15, 30301 (2025). doi: 10.1038/s41598-025-09986-w

24. Chen, H., Wang, W., Jia, L. & Wang, C. Research on time-varying path optimization for multi-vehicle type fresh food logistics distribution considering energy consumption. Sci. Rep. 14, 27068 (2024). doi: https://doi.org/10.1038/s41598-024-78639-1
25. Lyu, M., Li, L. & Liu, W. Multi-service network design with multi-function drones: Urban monitoring, data collection, and parcel delivery services. Transp. Res. Part C Emerg. Technol. 187, 105660 (2026). https://doi.org/10.1016/j.trc.2026.105660
26. Hosseini Dolatabadi, S. H., Bhuiyan, T. H., Kaleem, W., Subramanyam, A. & Cokyasar, T. A branch-and-cut algorithm for routing a heterogeneous drone-ground vehicle fleet to deliver time-sensitive products. Transp. Res. Part C Emerg. Technol. 183, 105454 (2026). https://doi.org/10.1016/j.trc.2025.105454
27. Hasan, S., Sheltami, T. & Mahmoud, A. Traffic-predictive drone scheduling: Day-ahead synchronization of mobile depots and parallel aerial sorties in urban airspace. Drones 10, 461 (2026). https://doi.org/10.3390/drones10060461
28. X. -B. Wu, X. -Y. Zhang, and X. -Q. Li, "Measurement, Regional Differences and Influencing Factors of Commercial Development Level in the Guangdong-Hong Kong-Macao Greater Bay Area from the Perspective of POI Big Data," Industrial Innovation Research, 2024.
29. Paul, A., Levin, M. W., Waller, S. T. & Rey, D. Data-driven optimization for drone delivery service planning with online demand. Transp. Res. Part E Logist. Transp. Rev. 198, 104095 (2025). https://doi.org/10.1016/j.tre.2025.104095

Funding

This research was funded by Guangxi Science and Technology Base and Talent Project for Guangxi Science and Technology Plan Project: Construction of Guangxi Transportation New Technology Transfer Center Platform (No. Guike AD23026029) , Construction of Scientific and Technological Innovation Bases for Science Research and Technology Development Plan Project of Nanning City: Intelligent Operation and Maintenance of Transportation Infrastructure and Health Monitoring Platform (No. 20223230) .

Author contributions

Guobin Gu: Conceptualization, Methodology.Longtang Ning: Validation, Formal analysis.Benxiao Lou: Software, Resources.Qinwei Hu: Investigation, Data curation.Junhui Luo: Writing – original draft, Visualization.Shixuan Zhou: Writing – review & editing, Supervision.BOONSUB PANICHAKARN: Project administration, Funding acquisition.

All authors reviewed the final manuscript and approved it for publication.

Competing interests

The authors declare that they have no conflicts of interest.